한국기계가공학회지, 제18권, 제1호, pp.16～23(2019.01) ISSN 1598-6721(Print)
Journal of the Korean Society of Manufacturing Process Engineers, Vol. 18, No. 1, pp.16~23(2019.01) ISSN 2288-0771(Online)

https://doi.org/10.14775/ksmpe.2019.18.1.016

A Study on the Collecting Efficiency of Oil-mist Filter according to the Sub-filter Shape

Yong Sun Kim*, Seong Min Yun*, Hee Jae Shin**, Sang Cheol Ko***,#
*Graduate School, Department of Mechanical Engineering, Jeonju UNIV,
**Institute of Carbon Technology, Jeonju UNIV,
***Department of Mechanical and Automotive Engineering, Jeonju UNIV.

서브필터 형상에 따른 Oil-mist Filter의 포집효율 향상에 관한 연구

김용선*, 윤성민*, 신희재**, 고상철***,#
*전주대학교 기계공학과,**전주대학교 탄소연구소,***전주대학교 기계자동차공학과
(Received 8 October 2018; received in revised form 4 November 2018; accepted 25 November 2018)

ABSTRACT

Cooking oil in kitchen-fog is the most harmful factor to the health of a cook. The proposed filter is a tool that protects the cooked state, to prevent users from inhaling oil mist in the kitchen. Due to efficiency issues, existing filters are of the mesh type or baffle type. In this paper, CFD analysis is carried out to select a filter with low pressure loss and low efficiency, and to attach the sub-filter to improve efficiency. The results of the analysis on the collection efficiency and pressure loss of three sub-filters, i.e., circle type, droplet type, and cone type, showed that the collection efficiency was 64.09% and the pressure loss was 1.26 mmAq when the circle type sub-filter was applied. The position of the sub-filter showed the best efficiency and pressure loss when it was located at the bottom of the center of the gap of the main filter.

Key Words : Oil-mist(유증기), Filter(필터), Computational Fluid Dynamics(전산유체역학), Fluid Flow(유동)

1. Introduction

In the residential spaces, the kitchen and the living room are interconnected in general. Thus, if the harmful substances generated in the kitchen are not properly discharged through the vents in the kitchen or other ventilation facilities, the quality of the indoor air will decrease, causing adverse effects on the human body. In the kitchen, which is a place that causes the generation of indoor air pollutants, oil mists generated in the cooking process can cause respiratory disease, asthma, respiratory disorder, etc.[1]

The kitchen hood removes these harmful substances. Therefore, the hood has a significant effect on the kitchen and indoor environment, and research on the filter to effectively remove oil mists from the kitchen is important.[2] The shape of the filters used in the kitchen has a significant effect on

Corresponding Author : scko@jj.ac.kr
Tel: +82-63-220-2623, Fax: +82-63-220-3161

their pressure loss and efficiency. The typical ones are mesh and baffle types. The mesh type causes almost no pressure loss, but its disadvantage is low oil mist collection efficiency. The baffle type has an advantage in collection efficiency, but its disadvantage is high pressure loss, which increases the capacity and vibration of the fan while sucking air. Various shapes of filters have already been analyzed, but most of them focused on the shape of the main filter.[3-7] The chevron type, which is a baffle type, showed a collection efficiency of 93% and a pressure loss of 6.35 mmAq in previous studies. Due to the high pressure loss, the fan requires high power and the workability of the shape is inefficient.

In this study, the workability of the chevron-type filter is improved by removing the protrusions that generate high pressure and simplifying the shape. In addition, the pressure loss is lowered and the collection efficiency is increased through computational fluid dynamics analysis. Variables are set according to the shape and location of the sub-filter, and a simplified sub-filter that can reduce the load on the fan by lowering the pressure loss is proposed.

2. Theoretical Background and Numerical Analysis Method

2.1 Turbulence Model

To calculate the collection efficiency and pressure loss of the filter, the $k-\omega\ SST$(Shear-Stress Transport) of ANSYS FLUENT 15.0 was selected as the turbulence model for this analysis, considering the importance of the flow near the wall.

The $k-\omega\ SST$ model combines the advantages of two models: the $k-\epsilon$ model, which can analyze the region of a low Reynolds number near the wall. Eq. (1) represents the kinetic energy k, and Eq. (2) represents the transport equation of the specific dissipation rate ω. D_ω in Eq. (2) is a cross-diffusion term. Near the wall, the k-ϵ model is used to predict the viscous effect properly, and inside the flow, the k-ϵ model is used for calculation.

$$\frac{\partial}{\partial t}(\rho k)+\frac{\partial}{\partial x_i}(\rho k u_i) = \frac{\partial}{\partial x_j}\left(\Gamma_k \frac{\partial k}{\partial x_j}\right)+\widetilde{G}_k-Y_k+S_k \quad (1)$$

$$\frac{\partial}{\partial t}(\rho \omega)+\frac{\partial}{\partial x_i}(\rho \omega u_i) = \frac{\partial}{\partial x_j}\left(\Gamma_\omega \frac{\partial \omega}{\partial x_j}\right)+G_w-Y_w+D_w+S_w \quad (2)$$

In the above equation, the viscous terms Γ_k and Γ_ω are defined by the strain rate and specific dissipation rate, instead of the Reynolds number, to reflect the transport effect of the turbulent stress. Y_k and Y_ϵ are dissipation terms applying the regression analysis (piecewise) method. In Eq. (1), $\widetilde{G}_k$, which is the generation term of k, represents a value corrected for the strain of the flow and the specific dissipation rate ω.[8]

2.2 Particle Collection Theory

In this study, the Lagrangian method is used to calculate the position of each particle moving in a flow field. The particle kinetic equation of the Lagrangian method is expressed as Eq. (3):

$$\frac{d\overrightarrow{u_p}}{dt} = F_D(\overrightarrow{u}-\overrightarrow{u_p}) + \frac{\overrightarrow{g_x}(\rho_p-\rho)}{\rho_p}+\overrightarrow{F_x} \quad (3)$$

Where the left term represents the inertia force generated when a velocity acts on a particle; on the right side, $F_D(u-u_p)$is the drag applied to the particle, $\overrightarrow{g_x}(\rho_p-\rho)/\rho_p$is the force of gravity and buoyancy, and $\overrightarrow{F_x}$ mainly represents the lift. In each equation, u is the fluid speed, u_p is the particle

speed, μ is the viscosity coefficient, ρ is the fluid density, and, ρ_p is the particle density.
The drag $F_D(u-u_p)$can be determined by Eq. (4), and $\overrightarrow{F_x}$ can be determined by Eq. (5).[9]

$$F_D = \frac{18\mu}{\rho_p d_p^2}\frac{C_D Re}{24} \tag{4}$$

$$F_x = \frac{1}{2}\frac{\rho}{\rho_p}\frac{d}{dt}(u-u_p) \tag{5}$$

When particles move along the streamline, they are captured by a filter due to the inertia of the particles. This is called inertial collision and can be expressed by the Stokes number as the ratio of the particle's stopping distance and the filter's diameter, as in Eq. (6) [10]:

$$S_{tk} = \frac{\tau U_0}{d} \tag{6}$$

where τ is the relaxation time after the particle moves out of the streamline and returns to the streamline again, which can be calculated by Eq. (7):

$$\tau = \frac{1}{18}\frac{d^2\rho_p}{\mu} \tag{7}$$

where U_0 is the initial speed of the particle and τU_0 is the shortest distance the particle moved for the relaxation time. A large S_{tk} means that there are many colliding particles, and the larger this value is, the greater the collection efficiency of the filter becomes. [9-11]

2.3 Analysis of Boundary Conditions and Basic Filter

One of the chevron-type filters was analyzed by simulation. Table 1 lists the basic properties of the air and oil mist for the flow analysis, and Table 2 lists the detailed boundary conditions for the filter analysis. Fig. 1 shows a simplified filter (S-filter) to which the existing chevron filter shape and the sub-filter have not been applied.

For this analysis, it was assumed that the droplet had a spherical shape and that droplets were uniformly sprayed in the inlet condition.

Fig. 2 shows the pressure distribution of the chevron filter and S-filter. The pressure loss of the chevron filter was relatively high at 6.35 mmAq, and the pressure loss of the S-filter was calculated as 0.94 mmAq.

Table 1 Basic physical properties of air and liquid

Fuild	Pattern	ρ_p (kg/m3)	ρ_{air} (kg/m3)	μ_g (kg/m·s)	μ_1 (kg/m·s)
Air-Liquid	Dispersed	980	1.225	0.0242	0.001

Table 2 Boundary conditions in CFD

	Chevron filter, S-filter
Filter frame width	100mm
Filter thickness	0.3 mm
Gap between filter	4.5 mm, 1.0 mm
Filter height	10 mm
Inlet (Particle, Air)	1 m/s
Particle size	1 ~ 10 μm

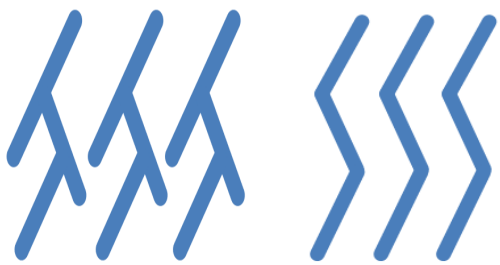

(a) Chevron filter **(b) S-filter**

Fig. 1 Filter of chevron type and S-filter

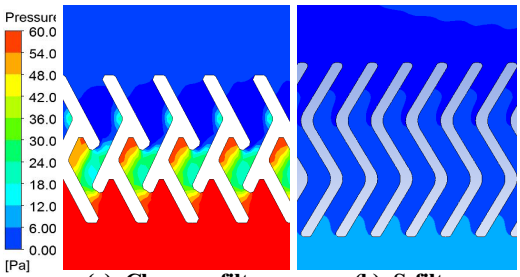

Fig. 2 Pressure contour of filter

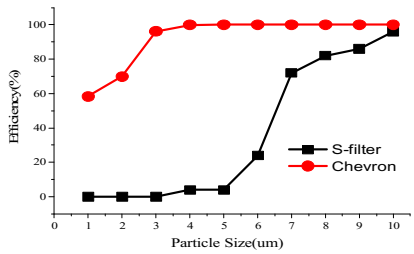

Fig. 3 Efficiency of the chevron filter

Fig. 3 shows the efficiencies of the chevron filter and S-filter. The chevron filter showed very high efficiency at 92.4%, but its pressure loss was large. The pressure loss of the S-filter was low, but its efficiency was 36.8%. The filters used in kitchens are generally designed with a pressure loss goal of 3 mmAq. or lower; thus, this study used a sub-filter to increase the efficiency.

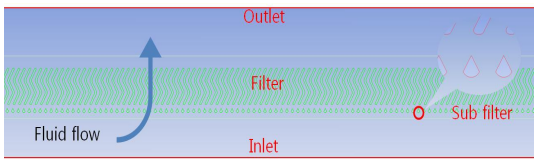

Fig. 4 Schematic of boundary conditions

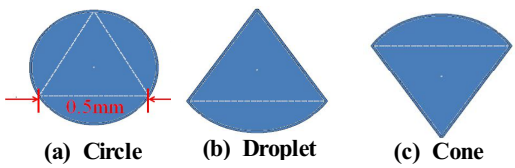

Fig. 5 Shape of sub-filter

2.4 Design of Sub-filter Shape

The boundary conditions applied to the numerical analysis to analyze the efficiency and pressure loss of the filter are shown in Fig. 4, and the three shapes selected for the sub-filter are shown in Fig. 5. The sub-filter was expected to play the role of a turbulence generator that generates turbulence in the incoming flow as the main filter.

A multiphase flow analysis was performed to examine oil mist and air simultaneously. The incoming mist was sprayed from the inlet and passed through the filter, and the mist that was not trapped was discharged through the outlet. The collection efficiency of the filter is expressed as Eq. (8).

$$Efficiency(\%) = \frac{Trap\ particle}{Total\ particle} \times 100 \quad (8)$$

To analyze the sub-filter according to its position, the filter was mounted at 1 mm in the –y direction from the main filter, and the efficiency was analyzed while moving it by 0, 0.25 mm, and 0.5 mm in the +x direction. Furthermore, each shape was drawn with the moved point as the center of a triangle.

3. Numerical Analysis Results

3.1 Analysis Result by Shape

Table 3 shows the total collection efficiency and pressure loss of the filter after applying the sub-filter and the speed of entering the bottom of the main filter. Fig. 6 shows the efficiency of each particle size for the three

Table 3 Efficiency by sub-filter type

Type	Efficiency (%)	Pressure loss (mmAq)	Velocity (m/s)
N/A	36.80	0.938	1.24
Circle	64.09	1.261	1.45
Droplet	63.78	1.142	1.44
Cone	61.32	1.140	1.40

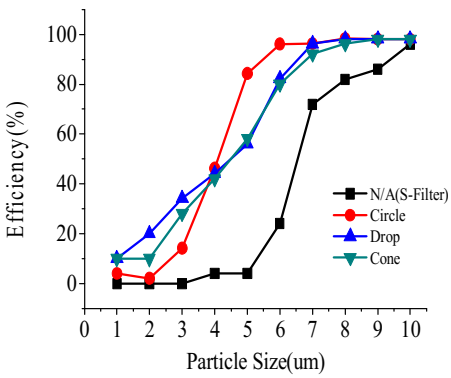

Fig. 6 Efficiency of filter with sub-filter

types of proposed filters. The analysis results confirmed that applying the sub-filter increased the collection efficiency. The circle showed the highest collection efficiency, followed by the droplet and the cone.

The pressure loss was 0.94 mmAq for N/A for no sub-filter and 1.26 mmAq for the circle. Thus, applying the sub-filter did not have a significant effect on pressure loss.

Fig. 7 shows the pressure distribution and vector components. The direction of the vortex in the wake of the sub-filter suggests that the sub-filter plays the role of a turbulence generator at the inlet of the main filter.

The efficiency increased as the speed increased because the Stokes number increased in proportion to the speed. When the Stokes number increases, the particles of inertial collision increase, which in turn increases the collection efficiency.[9-11]

3.2 Analysis Results by Position

The position of the sub-filter became a variable that controlled the turbulence component of the fluid entering the main filter. The basic position of the sub-filter was in the middle of the inlet of the main filter. Table 4 lists the collection efficiency, pressure loss, and the speed of the filter bottom when the fluid moved 0.25 mm in the +x direction. Fig. 8 shows the collection efficiency by particle size in a graph. When the sub-filter was moved 0.25 mm in the +x direction, the filter inlet speed decreased. The total collection efficiency decreased by 2.89%, 8.78%, and 4.72% for the circle, droplet, and cone types, respectively, and the pressure loss also decreased.

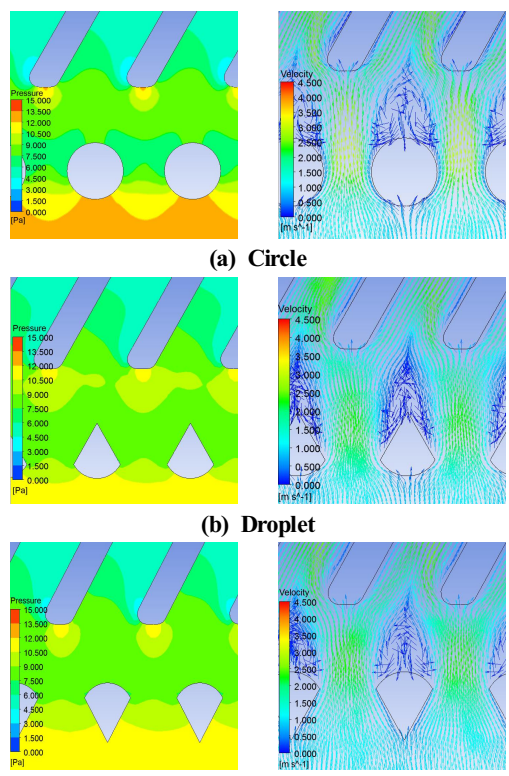

(a) Circle

(b) Droplet

(c) Cone

Fig. 7 Contour of filter with sub-filter
(Left : Pressure, Right : Vector)

Table 4 Efficiency by shift position 0.25mm

Shift 0.25mm	Efficiency (%)	Pressure loss (mmAq)	Velocity (m/s)
N/A	36.80	0.938	1.24
Circle	61.20	1.181	1.35
Droplet	56.60	1.120	1.31
Cone	55.00	1.100	1.31

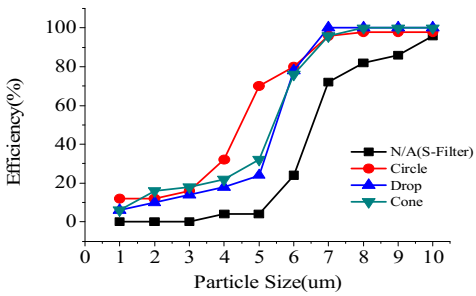

Fig. 8 Efficiency by sub-filter type(shift 0.25mm)

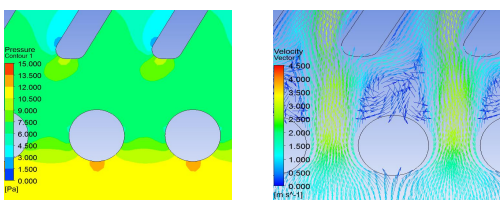

(a) Circle

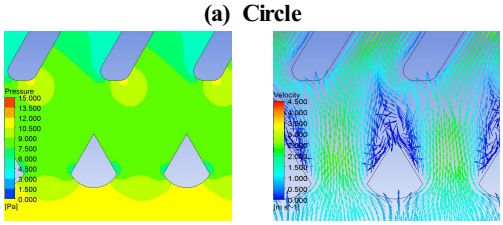

(b) Droplet

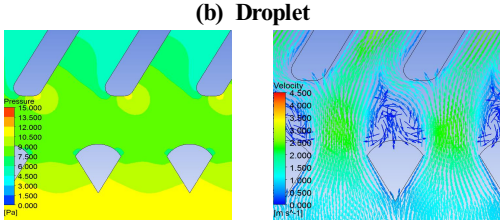

(c) Cone

Fig. 9 Contour of filter with sub-filter(shift 0.25mm) (Left : Pressure, Right : Vector)

Table 5 Efficiency by shift position 0.5mm

Shift 0.5mm	Efficiency (%)	Pressure loss (mmAq)	Velocity (m/s)
N/A	36.80	0.938	1.24
Circle	45.53	1.145	1.26
Droplet	48.43	1.006	1.28
Cone	41.60	1.005	1.25

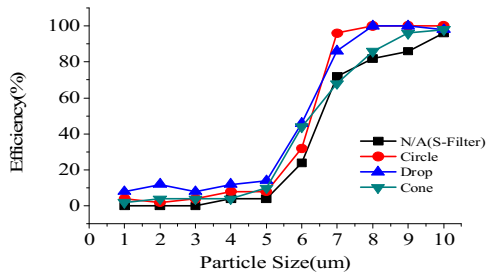

Fig. 10 Efficiency by sub-filter type(shift 0.5mm)

Fig. 9 shows the pressure distribution of the filter on the right and the vector component on the left.

The circle type showed the best efficiency when the fluid moved 0.25 mm as well. As the pressure interval changed, the speed and efficiency also decreased. Finally, regarding the collection efficiency and pressure when the fluid was moved 0.5 mm in the +x direction, since the gap of the main filter was 1 mm, when it moved 0.5 mm,it was located at the bottom of the main filter.

Table 5 shows the collection efficiency, pressure loss, and speed when the fluid moved 0.5 mm. Fig. 10 shows the total collection efficiency in a graph, and Fig. 11 shows the pressure and vector.

The sub-filter appears to have had almost no effect on controlling the flow into the bottom of the main filter because the sub-filter did not play its role as a turbulence generator. Furthermore, the sub-filter showed a lower collection efficiency of 3μm or smaller ultra-fine oil mist than the chevron filter. This is considered a problem in the inertial collection filter, and more variables are needed for a sub-filter or main filter shape to collect ultra-fine dust.

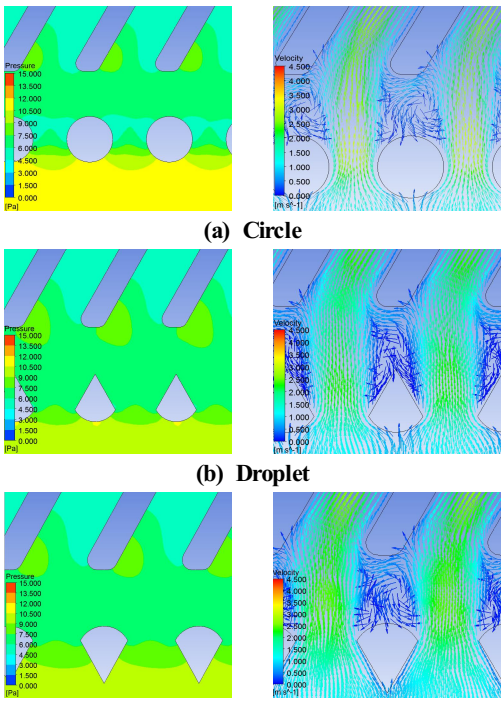

(a) Circle

(b) Droplet

(c) Cone

Fig. 11 Contour of filter with sub-filter(shift 0.5mm) (Left : Pressure, Right : Vector)

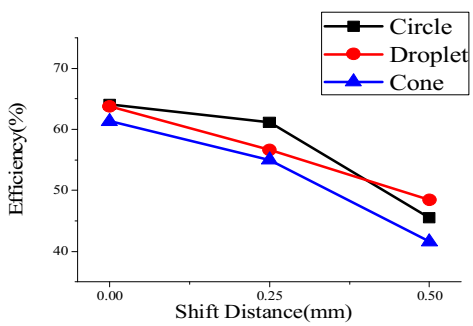

Fig. 12 Efficiency of collection by shift distance

Fig. 12 shows the total collection efficiency of each filter by distance. A tendency of lowering the collection efficiency with a longer distance can be seen. When the sub-filter was the circle type, the highest efficiency was obtained when it was located at the bottom center of the inlet of the main filter.

4. Conclusions

A numerical analysis was conducted according to different sub-filter shapes to increase the efficiency of the main filter. The results confirmed that the filter efficiency was increased just by mounting a sub-filter to play the role of a turbulence generator.

(1) The collection efficiency increased as the turbulence component of the sub-filter wake was changed. The efficiency was increased by the increased speed because the collection efficiency was increased as the dimensionless variable called the Stokes number was increased by the inertial collision in the particle collection efficiency.

(2) The streamlined circle shape of the sub-filter was effective at increasing the collection efficiency. It increased the collection efficiency by 27.8% compared with the S-filter, and the pressure loss increased by 0.32 mmAq.

(3) The best position of the sub-filter for efficient particle collection was at the bottom center of the inlet of the main filter. The circle type increased the collection efficiency by 15.7% at the 0 mm position compared with the 0.5 mm position.

(4) The filter with a sub-filter had lower collection efficiency for ultra-fine oil mist smaller than 3μm. To address this problem, more variables are required for the existing main filter and sub-filter shapes.

Acknowledgements

This study is a basic research project (No. 2016R1A6A1A03012069) conducted with the support of the Korea Research Foundation with funding from the Basic Science and Engineering Research

Project 2017 (NRF-2017R1D1A1B03036070) of the Korea Research Foundation and government funding (Ministry of Education) for 2016.

REFERENCES

1. Kim, Y. J., Kang, I. K., Byun, H. S., “Development Trend of Nanofiber Filter”, Membrane Journal, Vol. 16, No. 1, pp. 1-8, 2006.
2. Sohn, D. Y., Lim, J. H., Choi, Y. H., Park, J. H., “A Numerical Study on the Performance Improvement of Kitchen Range Hood by Air Induction and Air Curtain”, Korean Journal of Air-Conditioning and Refrigeration Engineering, Vol. 19, No. 4, pp. 321-327, 2007.
3. Kim, H. G., “New Design of Cap Type Filter for Oil Mist Removal”, Korean Society of Manufacturing Technology Engineers, Vol. 20, No. 1, pp. 13~16, 2011.
4. Choi, S. H., Lee, G. T., “An Experimental Study on the Kitchen Ventilation System Effectiveness by Character of Static Pressure Loss of Each System Component in Apartment Building”, JOURNAL OF THE ARCHITECTURAL INSTITUTE OF KOREA Planning & Design, Vol. 28, No. 3, pp. 269-276, 2012
5. Kim, K. J., Bae, G. N., Kim, Y. I., Hur, N. K., “ Numerical Study on the Design of a Grease Filter for Kitchen Ventilation”, Korean Journal of Air-Conditioning and Refrigeration Engineering, Vol. 15, No. 8, pp. 619-630, 2003
6. Park, J. C., “A Study on the Improvement Strategies for Exhaust Performance in Commercial Kitchen Hoods”, Korean Journal of Air-Conditioning and Refrigeration Engineering, Vol. 15, No. 5, pp. 439-445, 2003
7. Jang. S. C., Kim. J. W., Yi. C. S., “Numerical analysis on the inner flow characteristic for small smoke collector”, Journal of the Korean Society of Manufacturing Process Engineers, Vol. 12, No. 5, pp. 67-75, 2013.
8. VERSTEEG, H. K., Malalasekera, W., “An Introduction to Computational Fluid Dynamics: The Finite Volume Method”, Hongrung publisher. pp. 97-101, 2015
9. Kim, T. Y., Kim, H. G., “Analysis of Particle Matters by Using CFD Method in Indoor Environment”, Prospectives of Industrial Chemistry, Vol. 21, No. 2, pp. 9-15, 2018
10. Kim, K. J., Bae, G. N., Kim, Y. I., Hur, N. K., “A Numerical Study on the Particle Collection Characteristics of a Grease Filter for Kitchen Ventilation”, Korean Journal of Air-Conditioning and Refrigeration Engineering, Vol. 15, No. 10, pp. 792-801, 2002.
11. Ahn, J. H., Ahn, K. H., “Numerical Study of Particle Motion and Particle Beam Formation Through a Critical Orifice”, Transactions of the Korean Society of Mechanical Engineers – B, Vol. 23, No. 10, pp. 1240–1247, 1999.